Thermal Conductivity of the Iron-Based Superconductor FeSe: Nodeless Gap with a Strong Two-Band Character

P. Bourgeois-Hope,[1] S. Chi,[2] D. A. Bonn,[2,3] R. Liang,[2,3] W. N. Hardy,[2,3] T. Wolf,[4] C. Meingast,[4] N. Doiron-Leyraud,[1] and Louis Taillefer[1,3,*]

[1]*Département de physique and RQMP, Université de Sherbrooke, Sherbrooke, Québec J1K 2R1, Canada*
[2]*Department of Physics and Astronomy, University of British Columbia, Vancouver, British Columbia V6T 1Z1, Canada*
[3]*Canadian Institute for Advanced Research, Toronto, Ontario M5G 1Z8, Canada*
[4]*Institute of Solid State Physics (IFP), Karlsruhe Institute of Technology, D-76021 Karlsruhe, Germany*

(Received 22 March 2016; published 26 August 2016)

The thermal conductivity κ of the iron-based superconductor FeSe was measured at temperatures down to 75 mK in magnetic fields up to 17 T. In a zero magnetic field, the electronic residual linear term in the $T = 0$ K limit, κ_0/T, is vanishingly small. The application of a magnetic field B causes an exponential increase in κ_0/T initially. Those two observations show that there are no zero-energy quasiparticles that carry heat and therefore no nodes in the superconducting gap of FeSe. The full field dependence of κ_0/T has the classic two-step shape of a two-band superconductor: a first rise at very low field, with a characteristic field $B^\star \ll B_{c2}$, and then a second rise up to the upper critical field B_{c2}. This shows that the superconducting gap is very small (but finite) on one of the pockets in the Fermi surface of FeSe. We estimate that the minimum value of the gap, $\Delta_{\rm min}$, is an order of magnitude smaller than the maximum value, $\Delta_{\rm max}$.

DOI: 10.1103/PhysRevLett.117.097003

Amongst iron-based superconductors, the simple material FeSe has attracted much attention because, when made in thin-film form, its superconductivity appears to persist to a critical temperature $T_c \simeq 100$ K [1]. In bulk form, FeSe is unusual in that it undergoes the standard tetragonal-to-orthorhombic structural transition without the usual accompanying antiferromagnetic transition [2,3]. This raises fundamental questions about the role of magnetism in causing superconductivity and nematicity.

A basic property of any superconductor is its gap structure, which is related to the symmetry of its pairing state. Theoretical calculations for FeSe within a model where pairing proceeds via spin excitations yield a superconducting gap with accidental nodes on one of the Fermi surface pockets [4]. However, experimentally, there is no consensus on the gap structure of FeSe. A thermal conductivity study of nonstoichiometric $FeSe_x$ revealed a small residual linear term at $T \to 0$ K, interpreted as evidence against nodes in the gap [5]. In a subsequent study on stoichiometric FeSe, a huge residual linear term was reported [6], viewed as evidence of nodes. Specific heat measurements down to $T = 0.5$ K show that there are low-lying excitations but cannot distinguish between nodes and just a small minimum gap [7]. A penetration depth study of nonstoichiometric $FeSe_x$ revealed a two-band behavior with a small minimum gap $\Delta_{\rm min}$ [8], whereas measurements on FeSe show a nearly linear temperature dependence [6], pointing to nodes. Scanning tunneling microscopy (STM) on films [9] and crystals [6] detects a V-shaped density of states at low energy, suggestive of nodes, but not always [10].

In this Letter, we investigate the gap structure of stoichiometric FeSe using thermal conductivity, a bulk probe of the superconducting gap highly sensitive to the presence or absence of nodes [11]. Measurements were performed on two single crystals, grown by two different groups, and the results are in excellent agreement. We find that the residual linear term in $\kappa(T)$ as $T \to 0$ K, κ_0/T, is negligible at $B = 0$ T and it rises exponentially with magnetic field B at first, clear evidence that there are no nodes in the gap. The full field dependence reveals a classic two-band behavior, with a very small gap on one part of the Fermi surface, an order of magnitude smaller than the large gap on the other Fermi surface. This small gap is responsible for low-energy quasiparticle excitations that will make the specific heat, penetration depth, and STM spectrum of FeSe appear nodal in character unless measured down to a very low temperature.

Methods.—High-purity stochiometric single crystals of FeSe were grown by vapor transport [12]. (Note that in the early study by Dong *et al.* [5], the samples of $FeSe_x$ were not stoichiometric, and this introduces some uncertainty as to what would be the intrinsic properties of FeSe.) Our sample A was prepared at the University of British Columbia in Vancouver, Canada; our sample B was prepared at Karlsruhe Institute of Technology in Karlsruhe, Germany. They have similar characteristics, with $T_c = 9.3$ K (A) and 8.6 K (B) (Fig. 1). The contacts were made using silver paste. The thermal conductivity was measured in a dilution refrigerator down to 75 mK ($\simeq T_c/100$), for a heat current in the basal plane of the orthorhombic crystal

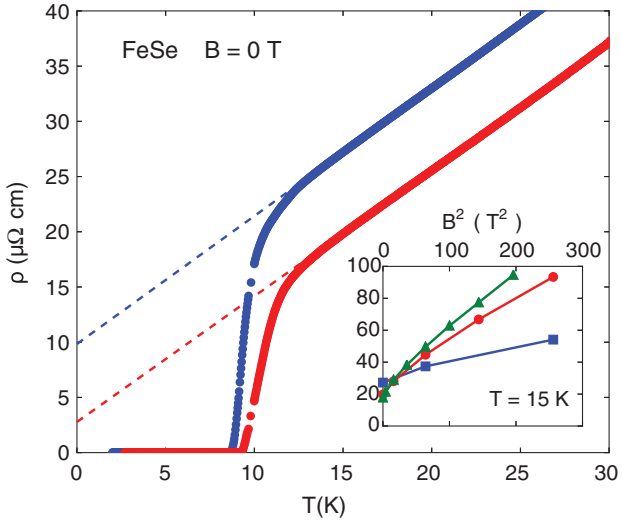

FIG. 1. In-plane electrical resistivity $\rho(T)$ of FeSe for our samples A (red) and B (blue). The dashed lines are a linear fit to $\rho(T)$ between 15 and 20 K, extended to $T = 0$ K, giving the residual resistivity $\rho(T \to 0\ \mathrm{K})$. (Inset) Dependence of ρ on magnetic field B, at $T = 15$ K, plotted as ρ vs B^2, for samples A (red circles) and B (blue squares), compared with corresponding data in Ref. [6] (green triangles).

structure, as described elsewhere [13]. A magnetic field up to 17 T was applied along the c axis and always changed at $T > T_c$.

Resistivity.—The in-plane resistivity $\rho(T)$ of our two samples is in excellent agreement with published data [6], when normalized to 410 $\mu\Omega\,\mathrm{cm}$ at $T = 300$ K. Differences are only visible when zooming at low temperature, as in Fig. 1. We see that the curve for sample B is shifted up relative to that of sample A, so that $\rho(T = 15\ \mathrm{K}) = 20.0\ \mu\Omega\,\mathrm{cm}$ (A) and $25.5\ \mu\Omega\,\mathrm{cm}$ (B). For comparison, the sample of FeSe in Ref. [6] has $T_c \simeq 9.4$ K and $\rho(T = 15\ \mathrm{K}) \simeq 18\ \mu\Omega\,\mathrm{cm}$, showing that its disorder level is similar to, perhaps slightly lower than, that of sample A. The sample of $FeSe_x$ in Ref. [5] has $T_c \simeq 8.8$ K and $\rho(T = 15\ \mathrm{K}) \simeq 80\ \mu\Omega\,\mathrm{cm}$, pointing to a much lower quality.

Owing to its semimetal-like Fermi surface made of small holelike and electronlike pockets, FeSe displays a strong orbital magnetoresistance (MR) [14], which goes approximately as $\rho(T \to 0\ \mathrm{K}) \propto B^2$. The level of disorder is likely to affect the magnitude of the MR, with lower disorder giving a larger MR. In the inset of Fig. 1, we compare the MR measured just above $T = 15$ K in our two samples and that of Ref. [6]. As expected, the MR increases with decreasing ρ.

Thermal conductivity.—The thermal conductivity $\kappa(T)$ of FeSe at low temperature is shown in the four panels of Fig. 2 for 26 different values of the magnetic field B, ranging from $B = 0$ T to $B = 17$ T. Data taken at $B = 1.5$, 3.0, 4.5, 6.0, 7.5, and 10.0 mT are not shown. At low field ($B < 1.0$ T), the data are well described by the form $\kappa/T = a + bT^2$ below $T \simeq 0.4$ K [Figs. 2(a) and 2(b)]. The residual linear term, $a \equiv \kappa_0/T$, is purely electronic, and the second term, bT^2, is due to phonon conduction [11]. In that regime, phonons are scattered by the sample boundaries, and the phonon mean free path is constant. In this Letter, our focus is entirely on κ_0/T, the electronic transport due to zero-energy quasiparticles. At higher field, $\kappa(T)$ gradually becomes more linear [Fig. 2(c)], as in the normal state above $B_{c2} = 14$ T [Fig. 2(d)]. In that regime, phonons are predominantly scattered by electrons, and their mean free path goes as $1/T$. Above 10 T, a fit to the form $\kappa/T = a + bT$ below $T \simeq 0.4$ K is used to extract κ_0/T [Figs. 2(c) and 2(d)].

At $B = 0$ T, $\kappa_0/T = 6 \pm 2\ \mu\mathrm{W/K^2\,cm}$ [Fig. 2(a)], a very small value. To put it in perspective, this value should be compared to the value in the normal state, κ_N/T, which we estimate by applying the Wiedemann-Franz law to the residual resistivity $\rho(T \to 0\ \mathrm{K}) = 2.8\ \mu\Omega\,\mathrm{cm}$ (Fig. 1), giving $\kappa_N/T = L_0/\rho(T \to 0\ \mathrm{K}) = 8.8\ \mathrm{mW/K^2\,cm}$, where

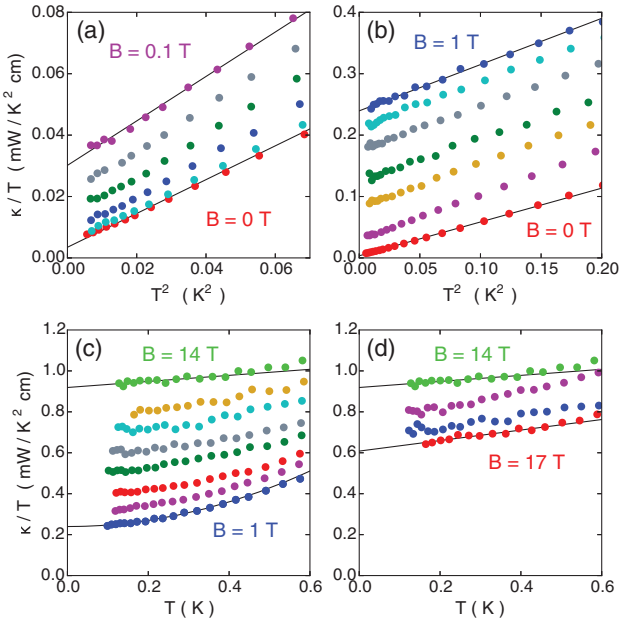

FIG. 2. Temperature dependence of the in-plane thermal conductivity $\kappa(T)$ of FeSe, measured on sample A, with an applied magnetic field $B \| c$. (a) Plotted as κ/T vs T^2 for $B = 0$, 0.02, 0.04, 0.06, 0.08, and 0.1 T (from bottom to top). Lines are a fit to $\kappa/T = a + bT^2$, used to obtain the residual linear term at $T = 0$ K, $a \equiv \kappa_0/T$. (b) Plotted as κ/T vs T^2 for $B = 0$, 0.1, 0.2, 0.3, 0.5, 0.75, and 1.0 T (from bottom to top). Lines are a fit to $\kappa/T = a + bT^2$. (c) Plotted as κ/T vs T for $B = 1$, 2, 4, 8, 10, 12, 13, and 14 T (from bottom to top). The lower line is a fit to $\kappa/T = a + bT^2$ ($B = 1$ T) and the upper line a fit to $\kappa/T = a + bT$ ($B = 14$ T). (d) Plotted as κ/T vs T for $B = 14$, 15, 16, and 17 T (from top to bottom). Lines are a fit to $\kappa/T = a + bT$. The values of $a \equiv \kappa_0/T$ obtained from a fit to either $\kappa/T = a + bT^2$ ($B < 11$ T) or $\kappa/T = a + bT$ ($B > 11$ T) are plotted as κ_0/T vs B in Fig. 3.

$L_0 \equiv (\pi^2/3)(k_B/e)^2$. We see that κ_0/T is ~0.07% of the normal-state conductivity, a negligible value. This shows that there are no zero-energy quasiparticles in the superconducting state of FeSe at $B = 0$ T. Note that the value reported in Ref. [5], $\kappa_0/T = 16 \pm 2$ μW/K^2 cm, is 4% of κ_N/T in their sample, a fraction similar to that found in KFe_2As_2 [15], a well-established nodal superconductor. By achieving a ratio $(\kappa_0/T)/(\kappa_N/T)$ 50 times smaller than in Ref. [5], our data make a compelling case for the absence of nodes.

The unambiguous confirmation for the absence of nodes comes by applying a magnetic field, a controlled way of exciting quasiparticles in the superconducting ground state at $T \simeq 0$ K. Looking at the full B dependence of κ_0/T up to 17 T [Fig. 3(a)], we see the typical behavior of a two-band superconductor like MgB_2 [16] or $NbSe_2$ [17]. Two features are striking. The first is the sharp cusp at $B = 14$ T. This is the upper critical field B_{c2}, below which vortices appear in the sample. The appearance of vortices introduces an additional scattering process, which suddenly curtails the mean free path, causing an abrupt drop in conductivity below B_{c2}, in samples with a long electronic mean free path. This happens in any clean type-II superconductor, whether the gap is nodeless—as in Nb or LiFeAs [18]—or nodal—as in KFe_2As_2 [15] or $YBa_2Cu_3O_y$ [19], provided the elastic normal-state mean free path is much longer than the $T = 0$ K coherence length ξ (i.e., the intervortex separation at B_{c2}) [20].

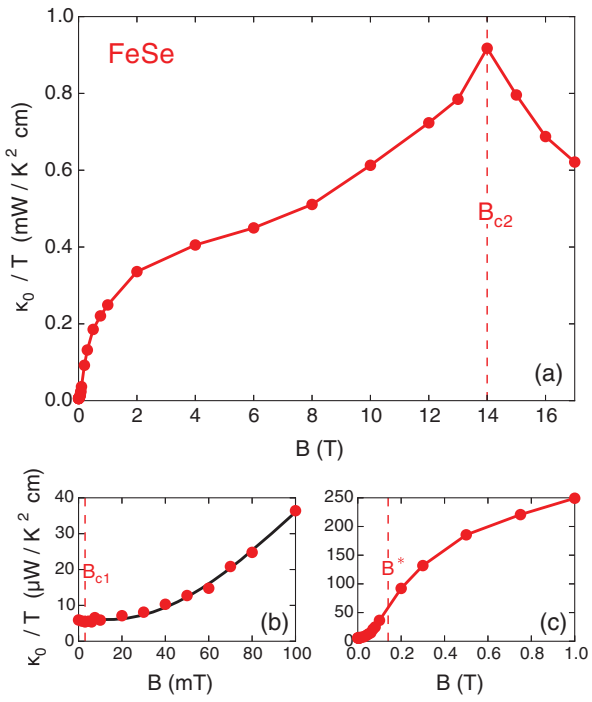

FIG. 3. Field dependence of the residual linear term κ_0/T in FeSe, obtained from fits to the data in Fig. 2. (a) Over the full field range. The vertical dashed line marks the upper critical field, $B_{c2} = 14$ T. (b) Zoom below $B = 0.1$ T. The vertical dashed line marks the lower critical field, $B_{c1} = 3$ mT [21]. The full line is an exponential fit to the data up to 0.1 T. (c) Zoom below $B = 1.0$ T. The vertical dashed line marks the inflection point from upward to downward curvature at $B^\star \simeq 150$ mT.

Note that the decrease in κ_0/T above B_{c2} [Fig. 3(a)] is due to the strong magnetoresistance of the normal state (inset of Fig. 1). As discussed below, the B dependence of κ_0/T is in quantitative agreement with the known B dependence of ρ [14]. This proves that the cusp indeed corresponds to the end of the vortex state and it rules out its previous interpretation as an internal phase transition inside the vortex state [6]. The values of B_{c2} thus obtained are 13.3 ± 0.2 T (Ref. [6]), 14.0 ± 0.2 T (sample A), and 15.2 ± 0.2 T (sample B).

The second striking feature of κ_0/T vs B is the rapid rise at low B [Fig. 3(a)]. To investigate this closely, the field was increased in very small steps, starting with $B = 1.5$ mT, then 3.0 mT, and so on [Fig. 3(b)]. In FeSe, the lower critical field above which vortices first enter the sample at $T \to 0$ K is $B_{c1} \simeq 3$ mT [21]. We find that increasing B up to 20 mT, a field 7 times larger than B_{c1}, causes little increase in quasiparticle conduction. This confirms that there are no nodes in the gap, for if there were, a field greater than B_{c1} would rapidly excite nodal quasiparticles, through the Volovik effect associated with vortices [20].

In Fig. 3(b), we see that the initial rise in κ_0/T vs B is exponential, so that the field-induced quasiparticle heat conduction in FeSe is an activated process (at low B), very different from the rapid rise characteristic of nodal superconductors [11,20]. This shows that there is a minimum gap for quasiparticle excitations; i.e., there are no nodes anywhere in the gap. However, that minimum gap (Δ_{min}) is much smaller than the maximum gap (Δ_{max}) responsible for setting B_{c2}. Indeed, the characteristic field for the initial rise is roughly $B^\star \simeq B_{c2}/100$, if we define $B^\star$ as the inflection point in κ_0/T vs B, where κ_0/T goes from a positive to a negative curvature [Fig. 3(c)], giving $B^\star \simeq 0.15$ T.

The quantity that controls how fast κ_0/T rises with B is not the superconducting gap Δ but the coherence length $\xi \propto v_F/\Delta$, where v_F is the Fermi velocity. In a single-band situation, the upper critical field is set by ξ: $B_{c2} \propto 1/\xi^2 \propto (\Delta/v_F)^2$. In a two-band model, the Fermi surface with the smaller ξ will set B_{c2}, while the surface with the larger ξ will control $B^\star$. In the two-band superconductor MgB_2, $B^\star \simeq B_{c2}/10$ because the small gap is 3 times smaller than the large gap [16]. Now, the Fermi surface of FeSe consists of two distinct pockets: a small Γ-centered hole pocket and a small electron pocket at the corner of the Brillouin zone [6,22]. Since the two pockets have comparable values of v_F [22], we conclude that the superconducting gaps on the two pockets differ by an order of magnitude.

Effect of disorder.—It is instructive to compare samples with different levels of disorder. In Fig. 4 (inset), we plot κ_0/T vs B, for samples A and B, at fields below $B = 1.0$ T. We see in sample B the same characteristics we saw in

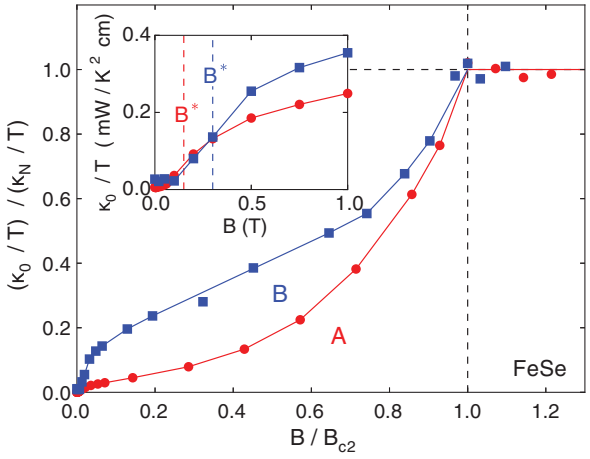

FIG. 4. Field dependence of the residual linear term κ_0/T in FeSe, comparing sample A (red circles) and sample B (blue squares). In the main panel, κ_0/T is normalized by the field-dependent normal-state conductivity κ_N/T (see the text) and B is normalized by B_{c2}. (Inset) Zoom of the raw data below $B = 1.0$ T. The color-coded vertical dashed lines mark the approximate location of the inflection point, separating a regime of upward curvature at low B and a regime of downward curvature at higher B, at $B^\star \simeq 0.15$ T (red) and $B^\star \simeq 0.3$ T (blue).

sample A: namely, a negligible κ_0/T at $B = 0$ T ($\simeq 1\%$ of κ_N/T), a flat κ_0/T at low B (up to $B \simeq 100$ mT), and a strong two-band character, with an inflection point at $B^\star \simeq 0.3$ T. So sample B leads us to the same qualitative conclusions: no nodes, but a very small gap on part of the Fermi surface. Quantitatively, the minimum gap appears to be larger, as measured by the larger value of $B^\star$. It therefore seems that disorder enhances the minimum gap. One way to interpret this is to invoke some gap anisotropy on the pocket with the small gap, so that $\Delta_{\rm min}$ is the minimum value of an angle-dependent gap. Disorder would then average out this anisotropy and cause $\Delta_{\rm min}$ to increase. Note that, because FeSe is orthorhombic, the gap function will involve a mixture of s-wave and d-wave components, which naturally introduces anisotropy [23].

It is then conceivable that in samples cleaner than sample A, the anisotropy is such that the deep minima further deepen to produce shallow accidental nodes where the gap changes sign [24]. This is the mechanism proposed by Kasahara *et al.* [6] to explain why they see a large residual κ_0/T in their clean sample of FeSe when a small residual term had instead been detected in the more disordered $FeSe_x$ [5]. Note, however, that the value of κ_0/T that they report at $B = 0$ T is enormous [6], 20–40 times larger than the value $\kappa_0/T \simeq 100$–200 mW/K^2 cm that we observe in both our samples just above $B^\star$ (Fig. 4 inset), and a sizable fraction of the total normal-state conductivity κ_N/T. Their enormous κ_0/T value at $B = 0$ T remains a puzzle.

In Fig. 4 (main panel), κ_0/T is normalized by the field-dependent normal-state conductivity, κ_N/T, and B is normalized by B_{c2}. We obtain κ_N/T by fitting the data points above B_{c2} to the relation $\kappa_N/T = L_0/(a + bB^2)$ since $\rho = a + bB^2$ in FeSe [14], given that $\kappa_N/T = L_0/\rho$ in the $T = 0$ K limit. For sample A, a fit to the data points at $B \geq 14$ T [Fig. 3(a)] yields $b \simeq 50$ nΩ cm/T^2, in agreement with the data in Ref. [14]. In Fig. 4, the data for sample B show a clear shoulder in $(\kappa_0/T)/(\kappa_N/T)$ at $B/B_{c2} \simeq 1/20$, similar to the shoulder seen in MgB_2 at $B/B_{c2} \simeq 1/9$ [16]. Our normalized data for κ_0/T vs B on sample B and A (Fig. 4) can be viewed as cleaner and much cleaner versions of the data in $FeSe_x$ [5], respectively, but they bear no resemblance to the data in Ref. [6].

Summary.—In summary, our thermal conductivity measurements on two high-quality crystals of FeSe reveal a superconducting gap without nodes, but with a strong two-band character, whereby the gap magnitude on one pocket of the Fermi surface of FeSe is an order of magnitude smaller than its magnitude on the other pocket. The presence of such a small gap will make various superconducting properties of FeSe, such as the specific heat and the penetration depth, appear as though they come from a nodal gap, unless measurements are carried out to very low temperature and/or very low energy.

We thank D. M. Broun, A. V. Chubukov, R. M. Fernandes and P. J. Hirschfeld for stimulating discussions. The work at Sherbrooke was supported by a Canada Research Chair, the Canadian Institute for Advanced Research (CIFAR), the National Science and Engineering Research Council of Canada (NSERC), the Fonds de recherche du Québec—Nature et Technologies (FRQNT), and the Canada Foundation for Innovation (CFI).

Note added.—Recently, three studies were reported that confirm our interpretation of a nodeless gap with a strong two-band character in FeSe, based on four different measurements: STM and specific heat [25], penetration depth [26,27], and microwave conductivity [27].

*louis.taillefer@usherbrooke.ca

[1] J.-F. Ge, Z.-L. Liu, C. Liu, C.-L. Gao, D. Qian, Q.-K. Xue, Y. Liu, and J.-F. Jia, Nat. Mater. **14**, 285 (2015).
[2] T. M. McQueen, A. J. Williams, P. W. Stephens, J. Tao, Y. Zhu, V. Ksenofontov, F. Casper, C. Felser, and R. J. Cava, Phys. Rev. Lett. **103**, 057002 (2009).
[3] M. Bendele, A. Amato, K. Conder, M. Elender, H. Keller, H.-H. Klauss, H. Luetkens, E. Pomjakushina, A. Raselli, and R. Khasanov, Phys. Rev. Lett. **104**, 087003 (2010).
[4] A. Kreisel, S. Mukherjee, P. J. Hirschfeld, and B. M. Andersen, Phys. Rev. B **92**, 224515 (2015).
[5] J. K. Dong, T. Y. Guan, S. Y. Zhou, X. Qiu, L. Ding, C. Zhang, U. Patel, Z. L. Xiao, and S. Y. Li, Phys. Rev. B **80**, 024518 (2009).
[6] S. Kasahara *et al.*, Proc. Natl. Acad. Sci. U.S.A. **111**, 16309 (2014).
[7] J.-Y. Lin, Y. S. Hsieh, D. A. Chareev, A. N. Vasiliev, Y. Parsons, and H. D. Yang, Phys. Rev. B **84**, 220507(R) (2011).

[8] R. Khasanov, M. Bendele, A. Amato, K. Conder, H. Keller, H.-H. Klauss, H. Luetkens, and E. Pomjakushina, Phys. Rev. Lett. **104**, 087004 (2010).
[9] C. Song *et al.*, Science **332**, 1410 (2011).
[10] T. Watashige *et al.*, Phys. Rev. X **5**, 031022 (2015).
[11] H. Shakeripour, C Petrovic, and L. Taillefer, New J. Phys. **11**, 055065 (2009).
[12] A. E. Böhmer, F. Hardy, F. Eilers, D. Ernst, P. Adelmann, P. Schweiss, T. Wolf, and C. Meingast, Phys. Rev. B **87**, 180505(R) (2013).
[13] J.-Ph. Reid, M. A. Tanatar, X. G. Luo, H. Shakeripour, N. Doiron-Leyraud, N. Ni, S. L. Bud'ko, P. C. Canfield, R. Prozorov, and L. Taillefer, Phys. Rev. B **82**, 064501 (2010).
[14] W. D. Watson *et al.*, Phys. Rev. Lett. **115**, 027006 (2015).
[15] J. Ph. Reid *et al.*, Phys. Rev. Lett. **109**, 087001 (2012).
[16] A. V. Sologubenko, J. Jun, S. M. Kazakov, J. Karpinski, and H. R. Ott, Phys. Rev. B **66**, 014504 (2002).
[17] E. Boaknin *et al.*, Phys. Rev. Lett. **90**, 117003 (2003).
[18] M. A. Tanatar *et al.*, Phys. Rev. B **84**, 054507 (2011).
[19] G. Grissonnanche *et al.*, Nat. Commun. **5**, 3280 (2014).
[20] I. Vekhter and A. Houghton, Phys. Rev. Lett. **83**, 4626 (1999).
[21] M. Abdel-Hafiez, J. Ge, A. N. Vasiliev, D. A. Chareev, J. Van de Vondel, V. V. Moshchalkov, and A. V. Silhanek, Phys. Rev. B **88**, 174512 (2013).
[22] T. Terashima *et al.*, Phys. Rev. B **90**, 144517 (2014).
[23] J. Kang, A. F. Kemper, and R. M. Fernandes, Phys. Rev. Lett. **113**, 217001 (2014).
[24] V. Mishra, G. Boyd, S. Graser, T. Maier, P. J. Hirschfeld, and D. J. Scalapino, Phys. Rev. B **79**, 094512 (2009).
[25] L. Jiao *et al.*, arXiv:1605.01908.
[26] S. Teknowijoyo *et al.*, arXiv:1605.04170.
[27] M. Li, N. R. Lee-Hone, S. Chi, R. Liang, W. N. Hardy, D. A. Bonn, E. Girt and D. M. Broun, New J. Phys. **18**, 082001 (2016).